Chaos, Solitons and Fractals 161 (2022) 112350

Contents lists available at ScienceDirect

Chaos, Solitons and Fractals

Nonlinear Science, and Nonequilibrium and Complex Phenomena

journal homepage: www.elsevier.com/locate/chaos

A dome subjected to compression forces: A comparison study between the mathematical model, the catenary rotation surface and the paraboloid

Rafael López

Departamento de Geometría Y Topología, Universidad de Granada, 18071 Granada, Spain

ARTICLE INFO

Article history:
Received 16 January 2022
Received in revised form 4 June 2022
Accepted 14 June 2022
Available online xxxx

Keywords:
Center of gravity
Singular minimal surface
Rotational tectum
Catenary rotation surface
Paraboloid

ABSTRACT

Singular minimal surfaces are models in architecture of domes where compression forces are the only ones acting on the dome. This paper investigates if catenary rotation surfaces and paraboloids are good candidates to substitute the singular minimal surfaces as designs for the construction of domes. Assuming that these surfaces have the same surface area and the same boundary curve, a numerical comparison of the heights of their centers of gravity and the curvatures is presented. This method is performed with *Mathematica* together with an analysis based on the slope linear regression line. The numerical results demonstrate that the centers of gravity of the two candidates are considerably close to that of the mathematical model. It is also proved that the paraboloids adjust better than catenary rotation surfaces.

1991 Mathematics Subject Classification

53Z30
53A10
68N30

1. Introduction

The shape of a hanging homogeneous flexible chain of given length and suspended from its ends has attracted the interest of scientists since the times of Leonardo *Da* Vinci and Galileo. Johann Bernouilli, Leibniz and Huygens gave separately an answer to a challenge proposed by Jacob Bernouilli asking what curve describes the shape of a hanging chain. The solution is the catenary

$$y(x) = \frac{1}{c}\cosh(cx+d), \quad c,d\in\mathbb{R}, c>0. \tag{1}$$

Under ideal hypotheses, the only forces acting on the chain are tangential, hence if its shape is inverted, these forces convert into compression forces. As a consequence, the catenary can be used as a model for the construction of arches [4,16,21,30]. The Spanish architect Antonio Gaud (1852–1926) used catenaries in many of his projects, especially in the construction of corridors (Fig. 1, left). For these corridors, he inverted a vertical catenary and repeated its shape along a horizontal direction. In the real world, arches are subjected to a variety of forces other than its own weight. This is the case of the cables of a suspended bridge as the Golden Gate Bridge at San Francisco. The weight of the road is very considerable in comparison with that of the cables. The curve that models the cables is the parabola $y(x) = cx^2 + d, c, d \in \mathbb{R}$. According to [36], funicular forms are the shapes that the structures adopt when only tension or compression forces are induced by loading. Catenaries and parabolas are examples of funicular shapes. Although these curves are similar at small scales, both curves are very different when one moves far from the lowest point because the catenary has an exponential growth whereas that of the parabola is quadratic.

A natural problem is to study the analogue of the catenary in dimension 2, that is, to investigate the shape of a surface suspended by its weight. Let $\mathbb{R}^3$ be the 3-dimensional Euclidean space with Cartesian coordinates (x,y,z) and denote by $\langle\cdot,\cdot\rangle$ the Euclidean product of $\mathbb{R}^3$. As usually, the z-axis will represent the vertical direction and the gravity will act on the negative direction of the z-axis. Consider a heavy uniform surface S of given area A_0 and spanned by a closed curve Γ. Assume that the only force exerted on S is the gravity. Then the equation that governs the shape of S in static equilibrium is

E-mail address: RCAMINO@UGR.ES (R. López).

https://doi.org/10.1016/j.chaos.2022.112350

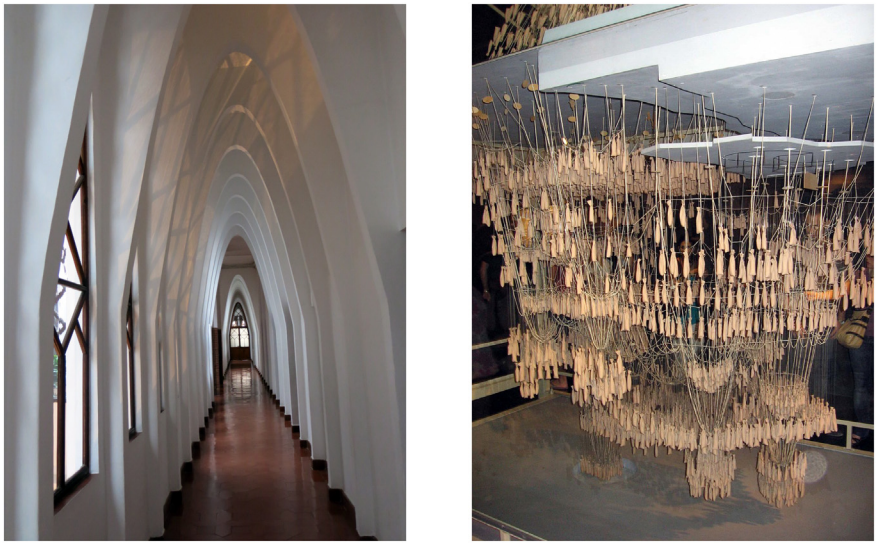

Fig. 1. Left: Corridor in the Colegio Teresiano, Barcelona [41]. Right: a hanging model of the church of Colonia Güell used by Gaud with funicular structures [42].

$$2H(p) = \frac{\langle N(p), e_3\rangle}{\langle p, e_3\rangle}, \quad p \in S, \tag{2}$$

where H is the mean curvature of S, N is the unit normal vector to S and $e_3 = (0,0,1)$. A surface is called *singular minimal surface* if satisfies [2] [6, 10,12].

Historically, many mathematicians were interested in the shape of a hanging surface, including Beltrami, Germain, Lagrange and Jellet [3,14, 18,22]. Poisson derived eq. (2) within of the theory of calculus of variations [33,p. 185]. A singular minimal surface is a model in architecture of a roof or a dome as the catenary is a model of an arch. The reason is similar because when S is suspended by its own weight, the only tension forces acting on S are tangent forces. In consequence, if S is inverted, then these forces are transformed into internal compression forces. This provides solidity in the construction and the risk of collapse and sagging is significantly diminished. In few words, the surface is a model of a 'perfect roof' according to the German architect Frei Otto [32].

A first example of solution of [2] is a vertical plane because $H = 0$ and $\langle N, e_3\rangle = 0$. Non-planar solutions of [2] can be found in the class of surfaces invariant along a direction $\vec{v}$. These surfaces are parameterized by $X(s,t) = \gamma(s) + t\vec{v}$, where $\gamma = \gamma(s)$, $s \in I \subset \mathbb{R}$, is a curve included in a plane orthogonal to $\vec{v}$. If, in addition, S is a singular minimal surface then $\vec{v}$ must be a horizontal vector. If γ is the graph of $z = z(x)$ situated the xz-plane, then $\vec{v} = (0,1,0)$ and the parameterization of the surface is $X(x,y) = (x,y,z(x))$. Then eq. (2) is

$$\frac{z''}{1+z'^2} = \frac{1}{z}.$$

This is the one-dimensional version of [2] whose solution is the catenary [1]. As a consequence, the mathematical model of a long corridor is a cylindrical surface whose section is a catenary. This is just what Gaud did in its constructions of corridors by repeating the shape of a vertical catenary [17,23]. As mathematical surfaces, the stability of long corridors has been recently investigated by the author [27].

Assuming a general geometry of the surface, it is not possible to find explicit solutions of [2] by quadratures. Although Gaud was unaware of the Poisson's work on hanging surfaces, he already suspected that their shapes were difficult to be described. That is why Gaud used models of hanging skeletons made by threads with small sand bags suspended from them (Fig. 1, right). Moving the vertices and changing the weights, he succeeded in finding approximated models of domes and roofs. Some of these models were later employed in the construction of the church of Parque Güell and Sagrada Familia (Barcelona). Antonio Gaud and Frei Otto were architects that found in nature the shapes of their designs, and both were part of the architectural movement called 'form finding'. Without to be a complete list, classical references in architecture about the constructions of domes are [7,8,15,28,39]. However, as far as the author knows, there is no literature on the employ of singular minimal surfaces for the construction of roofs and domes.

The organization of this paper is as follows. Section 2 presents the objectives of the paper and the definitions of the three surfaces of study. Section 3 gives a theoretical approach of singular minimal surfaces using calculus of variations, together with a description of those surfaces that are of rotational type. Next, the heights of the centers of gravity of catenary rotation surfaces and paraboloids are compared in relation with that of singular minimal surfaces (Sections 4 and 5, respectively). The results of these computations appear at the end of each section. In Section 6, the curvatures of the profile curves of the three surfaces are compared with each other. A discussion of conclusions is given in Section 7. Finally, an appendix shows the *Mathematica* codes utilized in the computations.

2. Objectives and definitions

This section is devoted to formulate the objectives of this paper together with the required definitions. The shape of a hanging surface is characterized for having the lowest center of gravity among all surfaces with the same boundary and the same area. The focus of this paper is domes with axial symmetry and all surfaces that will appear are axisymmetric with respect to the z-axis. Recall that this axis is the direction of the gravity. These surfaces of revolution are generated by the rotation with respect to the z-axis of planar curves contained in the coordinate xz-plane. In the next section, it will prove the existence of singular minimal surfaces of rotational type that do not intersect the rotation axis. These surfaces present a 'hole' around the z-axis. Thus these surfaces are not realistic domes and must be discarded.

Definition 2.1. Let S be an axisymmetric singular minimal surface with respect to the z-axis. The surface S is called a rotational tectum if S meets the rotation axis.

Rotational tectums are the models of perfect rotational domes because they have the lowest center of gravity. The objective of this

paper is to compare the heights of the centers of gravity of rotational tectums with another two rotational surfaces which, not being singular minimal surfaces, may be candidates for the construction of rotational domes. The first surface is motivated by the catenary.

Definition 2.2. A catenary rotation surface is the surface of revolution generated by rotating a vertical catenary with respect to its symmetry axis.

Therefore, if a bounded piece of a catenary rotation surface is spanned by a horizontal circle, its center of gravity must be situated in a higher position with respect to that of the rotational tectum with the same boundary curve and the same surface area.

Question 1. Is there a significant difference between the height of the centers of gravity of a rotational tectum and a catenary rotation surface?
The second candidate surface is the paraboloid, also known as elliptic paraboloid or paraboloid of revolution.

Definition 2.3. A paraboloid is the surface of revolution generated by rotating a vertical parabola with respect to its symmetry axis.

It is natural to consider paraboloids as candidates because the parabola is other funicular curve. Hence that the corresponding rotational surface generated by the parabola may be a good approximation of a dome.

Question 2. Is there a significant difference between the height of the centers of gravity of a rotational tectum and a paraboloid?
If the comparison between each one of the candidate surfaces with the mathematical model is one of the objectives, by the way, it is natural to compare both candidate surfaces.

Question 3. With respect to the centers of gravity, which surface, a catenary rotation surface or a paraboloid, is more accurate to the mathematical model of a rotational tectum?
The answer to these questions, or at least an investigation to compare the three surfaces, may have important implications in architecture. When a mathematical model is implemented to the construction of a building, the nature of the functions employed is crucial in the computations [29,34,35]. Going back to the three above surfaces, the mathematical model is governed by an axisymmetric solution of [2]. This equation is of second order and it is necessary numerical methods to solve it. The catenary rotation surface is constructed with the catenary [1] as profile curve, a curve determined by exponential functions, which are difficult to implement in practice. In contrast, the paraboloid is defined with a polynomial function, being the parabola much simpler than the catenary. In fact, the parabola is the simplest curve after a straight line because it is determined by a polynomial of degree 2.

The aim of the study is to investigate if the two candidate surfaces adjust to the mathematical model in the sense that their centers of gravity are closed or far from the mathematical model. The height of the center of gravity is, up to physical constants, the weight of the surface. However, despite the fact that rotational tectums, or in general, singular minimal surfaces are considered to be the mathematical model, a comparison study of the center of gravity with other surfaces has not been examined in the literature. To determine the center of gravity of the rotational tectum, it will be employed a numerical method with *Mathematica* [43] because the differential equation that governs this surface cannot be integrated by quadratures. In contrast, the centers of gravity of the two candidates can be explicitly calculated. Following Shah, Animasaun and Wakif et al., the statistical method of slope of linear regression line will be used to compare and discuss the results from the data obtained of the three surfaces [1,38,40].

Other parameters that will be investigated are the curvatures of these surfaces. On a mathematical surface as model in architecture, stresses due to elastic deformations are related to the curvatures of the surface. In general, high curvatures (small radius of curvature) are difficult to implement in real constructions. The surfaces studied in this paper are all surfaces of revolution, hence that it is interesting to investigate the curvature of the profile curve. An example is the study of the curvature at the vertex of the surface, which corresponds with the top of the dome after the surface is reversed.

3. Theoretical review

3.1. The Euler-Lagrange equation

This section presents the Euler-Lagrange equation of the variational problem associated to the problem of a hanging surface. Let Γ be a closed curve and let $S \subset \mathbb{R}^3$ be a compact surface S spanned by Γ. Suppose that S is made by an incompressible material with uniform density σ per unit of area. The area A_0 of S is fixed because it is assumed that the surface cannot be stretched. As physical assumptions, the only forces acting on S will be the force of gravity. After the presentation of the problem of the hanging surface. The question is what is the equation that describes the surface when it reaches a static equilibrium. To derive the Euler-Lagrange equation, the techniques of calculus of variations are employed. Since the problem is local, it suffices to assume that S is the graph of a function $u = u(x,y)$ defined in a bounded domain $\Omega \subset \mathbb{R}^2$, where $u_{|\partial\Omega}$ parameterizes the boundary curve Γ. The position of equilibrium is characterized by the fact that the center of gravity of S attains its lowest position. If the weight is measured with respect to the plane $z = 0$, then the height of the center of gravity is

$$\frac{\sigma g}{M}\int_\Omega u(x,y)\sqrt{1+u_x^2+u_y^2}\,dxdy, \tag{3}$$

where g is the gravitational acceleration and M is the mass of the curve. The subindices stand for the corresponding derivatives of the function u with respect to the variables x and y. Here it is assumed implicitly that S lies over the plane $z = 0$. The Lagrange multiplier of the area of S is

$$A_0 = \int_\Omega \sqrt{1+u_x^2+u_y^2}\,dxdy.$$

Define the functional

$$\begin{aligned} J[u] &= \frac{\sigma g}{M}\int_\Omega u\sqrt{1+|Du|^2}\,dxdy + \lambda\int_\Omega \sqrt{1+|Du|^2}\,dxdy \\ &= \int_\Omega \left(\frac{\sigma g}{M}u+\lambda\right)\sqrt{1+|Du|^2}\,dxdy, \end{aligned} \tag{4}$$

where $Du = (u_x, u_y)$ is the gradient of u and $\lambda \in \mathbb{R}$. Under an arbitrary infinitesimal variation $u(x,y) + t\varphi(x,y)$ of $u = u(x,y)$, where φ is smooth in Ω and $\varphi = 0$ along $\partial\Omega$, if the function u is a critical point of J then

$$\left.\frac{d}{dt}\right|_{t=0} J[u+t\varphi] = 0.$$

Using standard arguments, an integration by parts and the Fundamental Lemma of the calculus of variations, the Euler-Lagrange equation is

$$\left(\frac{u_x}{\sqrt{1+|Du|^2}}\right)_x + \left(\frac{u_y}{\sqrt{1+|Du|^2}}\right)_y = \frac{\sigma g/M}{(\sigma g/Mu+\lambda)\sqrt{1+|Du|^2}}. \tag{5}$$

To simplify the arguments, all physical constants σ, M and g will be assumed to be 1. The constant λ can be $\lambda = 0$ after a vertical translation of the surface. Thus eq. (5) reduces into

$$\operatorname{div}\frac{Du}{\sqrt{1+|Du|^2}} = \frac{1}{u\sqrt{1+|Du|^2}}. \tag{6}$$

In this equation, the left-hand side of [6] is just twice the mean curvature H of S. The right-hand side can be expressed in terms of the unit normal vector N of S because for a graph $z = u(x,y)$,

$$N = \frac{(-Du, 1)}{\sqrt{1+|Du|^2}}.$$

Definitively [6] is the nonparametric form of [2].

The Euler-Lagrange eq. (6) is the first order approach to the problem of minimization of the energy [3]. In general, the problem of finding minimizers for given area and boundary is open in all its generality. Motivated by Nitsche [31], the next example shows a family of surfaces with prescribed area and boundary whose center of gravity can be as lower as one desires (Fig. 2). Let Γ be a circle of radius 1 and contained in the plane P of equation $z = 0$. For each $0 < R \le 1$, define the surface $S_R = \Omega_R \cup C_R$, where $\Omega_R \subset P$ is the annulus $R^2 \le x^2 + y^2 \le 1$ and C_R is the cone $u(r) = -h(R-r)/R$ in polar coordinates, $0 \le r \le R$ and $h = \sqrt{2 + 1/R^2}$. All surfaces S_R share the same boundary Γ and the same area $A_0 = 2\pi$, but the height of the center of gravity of S_R is $-\frac{1+R^2}{6R}\sqrt{1+2R^2}$, which goes to $-\infty$ as $R \to 0$.

3.2. Rotational tectums

Let S be an axisymmetric singular minimal surface about the z-axis. Suppose that its generating curve is $x \mapsto (x, 0, u(x))$, where $u : I \subset \mathbb{R}^+ \to \mathbb{R}^+$ is a positive function. Consider the parameterization of S given by $X(x,\theta) = (x\cos\theta, x\sin\theta, u(x))$. Then [2] becomes

$$\frac{u''}{1+u'^2} + \frac{u'}{x} = \frac{1}{u}. \tag{7}$$

Comparing [7] with [6], the hypothesis on the axial symmetry makes that the eq. (6) converts into an ordinary differential equation. If $r_0 > 0$, standard theory implies local existence of solutions of [7] for any two initial conditions on $u(r_0)$ and $u'(r_0)$. A detailed description of the solutions of [7] appears in [9,11]. A class of solutions corresponds with curves that do not meet the rotation axis. These solutions have winglike shape and appear with the initial conditions $r_0 > 0$, $u(r_0) = z_0 > 0$ and $u'(r_0) = 0$ (Fig. 3, left).

The objects of study in this paper are those rotational surfaces that meet the z-axis, and thus, the intersection with this axis must be orthogonal (Fig. 3, right). However, eq. (7) is degenerated at $z = 0$ and standard theory does not ensure, in principle, local existence around this value. This can be overcome by using the fixed point theorem for Banach spaces, proving that eq. (7) has a solution for initial conditions

$$u(0) = z_0 > 0, \quad u'(0) = 0. \tag{8}$$

See [24] for details. The surface generated by this solution is a rotational tectum according to Definition 2.1. Another solution of [7] is $v(x) = x$ for $x > 0$, that is, a cone with vertex at the origin of coordinates. This surface does not meet the z-axis and its shape is a conical tent once inverted the surface. The most remarkable properties of the rotational tectums are [11]:

(1) The maximal domain of the solution is $[0,\infty)$.
(2) The function u is strictly increasing and presents a minimum at $x = 0$.
(3) The function u is asymptotic to the conical solution $v(x) = x$.

Rotational tectums are peculiar in the family of singular minimal surfaces in the following sense. It is natural to ask if there are other compact non-rotational singular minimal surfaces whose boundary is a horizontal circle. The answer is negative and given in the following result [25,26].

Proposition 3.1. Let S be a compact singular minimal surface without self-intersections. If the boundary of S is a horizontal circle, then S is a surface of revolution.

The hypothesis that the surface has not self-intersections is natural if one thinks in models of realistic domes. From the architectural viewpoint, this proposition says that if one wants to construct a dome with circular boundary, then the surface must be rotational. This is in concordance with the intuition that the axial symmetry of the boundary curve is inherited to the whole surface that spans.

4. Rotational tectums *versus* catenary rotation surfaces

4.1. Approach and methodology

This section is devoted to compare the centers of gravity of rotational tectums and catenary rotation surfaces having the same boundary curve and surface area. A rotational tectum $\mathcal{T}$ is generated by a solution $u = u(x)$ of (7)– [8]. Suppose that the boundary of $\mathcal{T}$ is the horizontal circle of radius $R > 0$

$$\Gamma_R = \left\{(x, y, h_0) : x^2 + y^2 = R^2\right\},$$

where $h_0 = u(R)$ is the height of the circle Γ_R. The area A_0 of $\mathcal{T}$ is

$$A_0 = 2\pi \int_0^R x\sqrt{1+u'^2}\,dx,$$

and the height h_T of its center of gravity is

$$h_T = \frac{2\pi}{A_0}\int_0^R xu\sqrt{1+u'^2}\,dx.$$

In the comparison analysis between both surfaces, it is enough to fix the position of one of them. To facilitate the computations, the rotational tectum will be fixed and next, the catenary rotation surface will be moved vertically until that the boundary curve and the area coincide

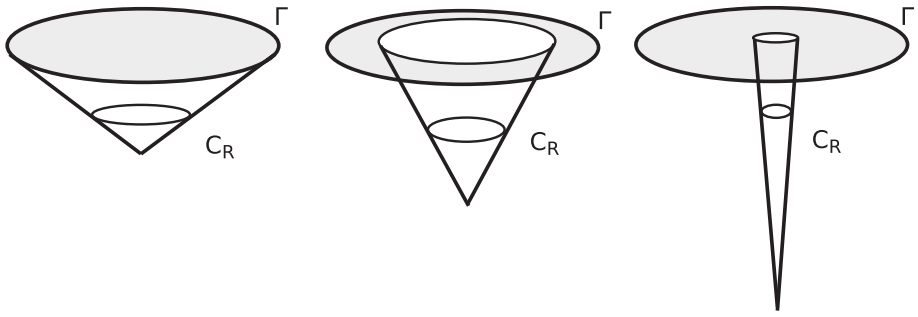

Fig. 2. A family of surfaces parameterized by R, where all surfaces have the same area and boundary, but the height of the center of gravity goes to $-\infty$ as $R \to 0$.

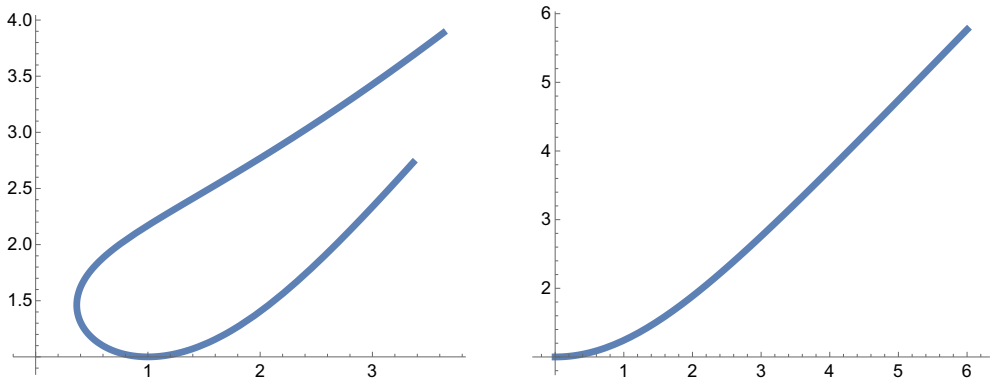

Fig. 3. Profiles curves of rotational singular minimal surfaces. Left: the initial condition are $u(1) = 1$ and $u'(1) = 0$ and the curve does not intersect the z-axis. Right: the initial conditions are $u(0) = 1$, $u'(0) = 0$ and the curve meets the z-axis (rotational tectum).

with that of $\mathcal{T}$. Consider the catenary [1] contained in the xz-plane where the z-axis is its axis of symmetry. This implies $d = 0$ in [1]. The equation of the catenary is

$$z_{c,m}(x) = \frac{1}{c}\cosh(cx) + m, \quad x \in [0, R], \tag{9}$$

where c, $m \in \mathbb{R}$ and $c > 0$. The rotation of this catenary with respect to the z-axis defines a catenary rotation surface denoted by $\mathcal{C}_{c,m}$. Notice that $\mathcal{C}_{c,m}$ is not a catenoid because a catenoid is generated when the catenary rotates about a horizontal axis that does not intersect the catenary. Take the parameters c and m in [9] so that the area of $\mathcal{C}_{c,m}$ is A_0 and its boundary is Γ_R. Since the boundary is Γ_R, a first condition is

$$\frac{1}{c}\cosh(cR) + m = h_0. \tag{10}$$

The area of $\mathcal{C}_{c,m}$ can be computed by quadratures, obtaining

$$A = 2\pi\int_0^R x\sqrt{1 + z'_{c,m}(x)^2}\,dx = \frac{2\pi(cR\sinh(cR) - \cosh(cR) + 1)}{c^2}. \tag{11}$$

Finally the height h_C of the center of gravity of $\mathcal{C}_{c,m}$ is

$$\begin{aligned} h_C &= \frac{2\pi}{A_0}\int_0^R x z_{c,m}(x)\sqrt{1 + z'_{c,m}(x)^2}\,dx \\ &= \frac{\pi\left(2c^2R^2 + 2cR\sinh(2cR) - \cosh(2cR) + 1\right)}{4c^3A_0} + m. \end{aligned} \tag{12}$$

According to this scheme, first the boundary Γ_R is prescribed and next, this provides the area A_0 of $\mathcal{T}$. The area A_0 and the height h_T of the center of gravity of the rotational tectum are calculated with *Mathematica*. Therefore, the methodology follows the next steps:

(1) Fix $z_0 > 0$ in [8], the lowest point of $\mathcal{T}$. By using the function NDSolve of *Mathematica*, solve the initial value problem (7)–[8]. The domain of the solution u is $[0, \infty)$.
(2) Fix $R > 0$. Restrict the function u to the interval $[0, R]$. This determines a compact rotational tectum $\mathcal{T}$. Let Γ_R be its boundary curve.
(3) Compute the area A_0 of $\mathcal{T}$ by using the function `NIntegrate` of *Mathematica*.
(4) Calculate the parameters c and m of $\mathcal{C}_{c,m}$ in such a way that the area of $\mathcal{C}_{c,m}$ is A_0 and its boundary is Γ_R. Here the function `FindRoot` of *Mathematica* solves the eqs. (10) and (11).
(5) Compute the values of the heights h_T and h_C. For h_T, the function NIntegrate of *Mathematica* is used and for h_C, the formula given in [12].

The value z_0 of the lowest point of the rotational tectum can be previously fixed after a dilation from the origin. This is because if $u = u(x)$ is a solution of [7], the function $v(x) = cu(x/c)$, $c > 0$, is also a solution of [7]. Thus, the value $z_0 = 1$ will be assumed in the initial condition (8).

In this paper, this process will be computed for the rotational tectums whose boundary is a circle of radius R, where R goes from 2 to 20 in increments of two. Table 1 shows the data corresponding to the mathematical model of the rotational tectum. In it, the values of the radius of the boundary curve Γ_R, the height h_0 of this curve, the area A_0 of the surface and its center of gravity are shown.

Table 2 shows the comparison of the values h_T and h_C. In order to conduct a suitable analysis, the deviation $h_C - h_T$ of the centers of gravity of both surfaces is computed in relation to the total height of the surface. The height of the surface is $u(R) - u(0)$.

Another useful information is the determination of the lowest points of the rotational tectums and the catenary rotation surfaces. These points are denoted by lw_T and lw_C, respectively. From the architectural viewpoint, the lowest point determines the height of the dome once is reversed the position of the surface. These heights are $u(R) - lw_T$ and $u(R) - lw_C$, respectively. Here $lw_T = z_0 = 1$ in all cases because $z_0 = 1$ in [8]. For $\mathcal{C}_{c,m}$, the value of lw_C occurs evaluating $z_{c,\,m}(x)$ at $x = 0$. Thus $lw_C = 1/c + m$. Table 2 presents the deviation $lw_C - lw_T$ in relation to the height of the rotational tectum, namely, $(lw_C - lw_T)/(u(R) - 1)$. These computations are shown in Table 3. Fig. 8 shows some pictures of rotational tectums and catenary rotation surfaces.

4.2. Analysis of results and discussion

Overall, differences of less than one decimal in Table 2 between the values h_T and h_C prove that the height h_C of the center of gravity of the catenary rotation surfaces is very close to the value h_T. The slope of the linear regression line through data points on Microsoft Excel has been used to compare the information between rotational tectums

Table 1
Values of R, h_0, A_0 and h_T for the rotational tectum when the lowest height is $z_0 = 1$.

R	$h_0 = u(R)$	A_0	h_T
2	1.8854	14.63	1.4773
4	3.7295	66.22	2.5786
6	5.7681	155.99	3.8651
8	7.8292	282.30	5.1997
10	9.8837	444.43	6.5477
12	11.9278	642.08	7.8989
14	13.9628	875.13	9.2498
16	15.9903	1143.55	10.5993
18	18.0120	1447.30	11.9471
20	20.0290	1786.39	13.2932

Table 2
Comparison of the values h_T, h_C and h_P together with the deviations with the height of the rotational tectum.

R	h_T	h_C	h_P	$\% \frac{h_C - h_T}{u(R) - z_0}$	$\% \frac{h_P - h_T}{u(R) - z_0}$
2	1.4773	1.4782	1.4778	0.0969	0.0482
4	2.5786	2.58811	2.5843	0.3488	0.2119
6	3.8651	3.8887	3.8805	0.4942	0.3232
8	5.1997	5.2377	5.2253	0.5573	0.3753
10	6.5477	6.5994	6.5830	0.5819	0.3975
12	7.8989	7.9632	7.9430	0.5891	0.4046
14	9.2498	9.3261	9.3023	0.5887	0.4057
16	10.5993	10.6870	10.6598	0.5849	0.4033
18	11.9471	12.0458	12.0152	0.5798	0.4002
20	13.2932	13.4025	13.3686	0.5744	0.3962
$\mathbf{S_{lp}}$	0.6639	0.6701	0.6682	0.0196	0.0150

and catenary rotation surfaces. This value may be useful when testing whether the slope of the regression line for the height of the center of gravity h_C is significantly different from h_T. Another interesting quantity is the relation of the difference $h_C - h_T$ and the height of the rotational tectum. In percentage, this deviation is very small. Fig. 4 shows some pictures of rotational tectums and catenary rotation surfaces with the same area and boundary. The list of conclusions of Tables 2 and 3 are now presented.

(1) As expected, the height h_C of the center of gravity of $\mathcal{C}_{c,m}$ is higher than h_T. The center of gravity h_T of the mathematical model $\mathcal{T}$ increases as $R \to \infty$ with a rate of increase of $S_{lp} = 0.6639$. The same occurs for the value h_C, where the rate is $S_{lp} = 0.6701$. The fact the both slopes almost coincide indicate the good approximation of the catenary rotation surface. In percentage, the error of h_C with respect to h_T is only of 0.93%.
(2) Taking in consideration the difference $h_C - h_T$ in relation with the total height of the rotational tectum $\mathcal{T}$, the deviation is less than 0.60% for all values of R. The rate of increase is $S_{lp} = 0.0196$.
(3) The deviation percentage $\frac{h_C - h_T}{u(R) - z_0}$ attains a maximum and next decreases. This is shown in Fig. 5. In view of it, the (circle) points fit to a parabola. The equation of this concave parabola is computed with Microsoft Excel, being $y(R) = -0.0031R^2 + 0.0887R + 0.0076$. The maximum is attained at the value $R = 14.30$. In Table 2, this value is $R \approx 12$.
(4) The value $lw_T = 1$ is always less than lw_C. This is understandable, although there is no an *a priori* relation between the centers of gravity and the lowest points.
(5) The deviation $lw_C - lw_T$ increases as $R \to \infty$ and it is significant. The rate of increase is $S_{lp} = 0.2782$. Thus the top of the (inverted) catenary rotation surface is clearly below than of the rotational tectum and this difference increases when $R \to \infty$. This is confirmed with the slope of the deviation rate $(lw_c - z_0/(u(R) - z_0)$, which is $S_{lp} = 1.0158$.

Table 3
Comparison of lw_C, lw_P and the deviations with respect to the height of the rotational tectum.

R	lw_C	$\% \frac{lw_C - z_0}{u(R) - z_0}$	lw_P	$\% \frac{lw_P - z_0}{u(R) - z_0}$
2	1.0452	5.1079	1.0318	3.5900
4	1.3236	11.8550	1.2565	9.3987
6	1.7781	16.3190	1.6501	13.6348
8	2.3128	19.2236	2.1270	16.5027
10	2.8847	21.2156	2.6442	18.5085
12	3.4751	22.6495	3.1822	19.9690
14	4.0751	23.7228	3.7313	21.0701
16	4.6803	24.5515	4.2866	21.9246
18	5.2883	25.2075	4.8453	22.6035
20	5.8976	25.7377	5.4059	23.1536
$\mathbf{S_{lp}}$	0.2782	1.0158	0.2516	0.9852

5. Rotational tectums *versus* paraboloids

5.1. Approach and methodology

This section compares rotational tectums and paraboloids. With the same effort, catenary rotation surfaces and paraboloids also are compared with each other. This will answer to Questions 2 and 3.

Regarding Question 3, it deserves to give an observation about the comparison between the centers of gravity of catenary rotation surfaces and paraboloids. Recall that in the problem of the hanging chain, the center of gravity of the catenary is lower than the one of parabola. However, *a priori* this property does not imply that the corresponding rotational surfaces preserve this property. This is due because the prescribed initial data are different in both situations. In the hanging surface, these data are the boundary curve Γ_R and the area A_0. In the hanging chain problem, the initial data are the ends of the curve and its length. If a catenary rotation surface and a paraboloid have the same boundary curve and area, the generating curves have the same endpoints. However, the lengths are different. In terms of the generating curve $y(x)$, this is equivalent to say that there is no a relation between the value $2\pi\int_a^b x\sqrt{1+y'^2}\,dx$ (surface area) and $\int_a^b \sqrt{1+y'^2}\,dx$ (length of the curve).

Consider the parabola of equation

$$p_{c,m}(x) = cx^2 + m, \quad x \in [0, R], \tag{13}$$

where $c, m \in \mathbb{R}$, $c > 0$ and situated in the coordinate xz-plane. Let $\mathcal{P}_{c,m}$ be the paraboloid generated by rotating $p_{c,\,m}$ about the z-axis and parameterized by $X(x,\theta) = (x\cos\theta, x\sin\theta, p_{c,\,m}(x))$, $x > 0$, $\theta \in \mathbb{R}$. The height of the center of gravity of $\mathcal{P}_{c,m}$ is denoted by h_P. Since the boundary of $\mathcal{P}_{c,m}$ is Γ_R, then $p_{c,\,m}(R) = h_0$ implies

$$cR^2 + m = h_0.$$

The area of $\mathcal{P}_{c,m}$ can be computed explicitly:

$$A_0 = 2\pi\int_0^R x\sqrt{1+p'_{c,m}(x)^2}\,dx = \frac{\pi\left(\left(4c^2R^2+1\right)^{3/2} - 1\right)}{6c^2}.$$

The value h_P of its center of gravity is computed again by quadratures, namely,

$$h_P = \frac{2\pi}{A_0}\int_0^R x p_{c,m}(x)\sqrt{1+p'_{c,m}(x)^2}\,dx = \frac{\pi\left(\left(6c^2R^2-1\right)\left(4c^2R^2+1\right)^{3/2}+1\right)}{60c^3A_0} + m.$$

All above quantities are polynomial in the variables c and R which is much manageable regarding the computational cost. In contrast, the analogue calculations [10], [11] and [12] for catenary rotation surfaces are given in terms of the exponential function. As a result of these computations, Table 2 shows the values of h_P. Table 3 gives the computations of the lowest point of the paraboloid, which coincides with the parameter m.

5.2. Analysis of results and discussion

The almost coincidence of the values h_T and h_P reveals that paraboloids are very accurate to the mathematical model in terms of the heights of centers of gravity. Fig. 6 shows some pictures of rotational tectums and paraboloids with the same area and boundary.

(1) As expected, the height h_P of the center of gravity of the paraboloid is higher that of the rotational tectum, but as it

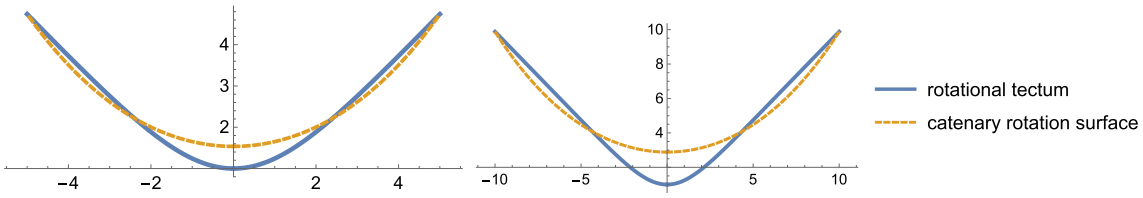

Fig. 4. Comparison between rotational tectums (thick) and catenary rotation surfaces (dashed). Left: $R = 5$ where $h_T = 3.2115$, $h_C = 3.2278$ an $lw_C = 1.5364$. Right: $R = 10$, $h_T = 6.5477$ and $h_C = 6.5994$. Here $lw_C = 2.8847$.

happened with the catenary rotation surface, the difference $h_P - h_T$ is very small. The rate of increase is $S_{lp} = 0.6682$. Comparing with the mathematical model, which is $S_{lp} = 0.6639$, the percentage error is only of 0.64 %.

(2) In terms of percentages in relation with the total height of the rotational tectum, the deviation $h_P - h_T$ is less than 0.41 % for all values of R. The rate of increase is $S_{lp} = 0.0150$.

(3) Regarding Question 3, the approximation of the paraboloid to the rotational tectum is better than the catenary rotation surface because $h_T < h_P < h_C$ for any R. This contrasts to the reverse property between the centers of gravity of the catenary and the parabola as previously mentioned. Table 2 shows that the increase is less than of the catenary rotation surface, being its rate of $S_{lp} = 0.0150$; for the catenary rotation surface is 0.0196.

(4) The deviation percentage $\frac{h_P - h_T}{u(R) - 1}$ increases until a maximum and decreases later. This behavior is similar than in the case of the catenary rotation surface. See (square) points in Fig. 5. Again, the polynomial regression that fits the deviation $\frac{h_P - h_T}{u(R) - 1}$ is of degree 2. Its equation is $y(R) = -0.0023R^2 + 0.0647R - 0.0273$ and its maximum attains at $R = 14.06$. This agrees closely with the value $R \approx 14$ obtained in Table 2.

(5) The value $lw_T = 1$ is less than lw_P. The difference $lw_P - lw_T$ is larger than $h_P - h_T$ and it increases if $R \to \infty$. However, this difference is less than in the case of catenary rotation surfaces. The rate of increase of lw_P in relation with the variable R is $S_{lp} = 0.2516$, and less than the value $S_{lp} = 0.2782$ for catenary rotation surfaces. This is also explained by comparing the slope or the linear regression line through the data of $\frac{lw_P - z_0}{u(R) - z_0}$ and $\frac{lw_C - z_0}{u(R) - z_0}$. For paraboloids, the slope of increase is $S_{lp} = 1.0158$, which is greater than the rate in the case of paraboloids, whose value is $S_{lp} = 0.9852$. This confirms again that paraboloids adjust better than catenary rotation surfaces.

(6) To summarize, the comparison between paraboloids and catenary rotation surfaces (using centers of gravity or deviation with respect to the total height) shows that paraboloid fit better than catenary rotation surfaces to the mathematical model.

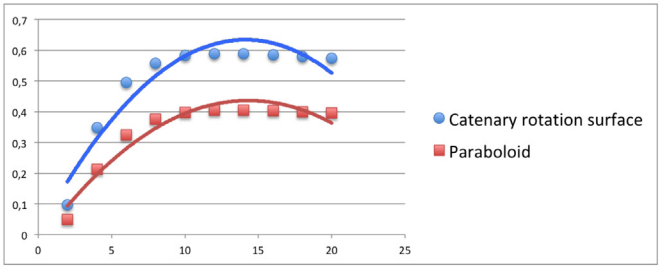

Fig. 5. Polynomial regression of second order adjusting the data points $\% \frac{h_C - h_T}{u(R) - z_0}$ and $\% \frac{h_P - h_T}{u(R) - z_0}$ of Table 2.

6. Comparing the curvatures along the profile curves

6.1. Approach and methodology

This section compares the curvatures of the three surfaces. The curvature κ of a planar curve $y = y(x)$ is

$$\kappa(x) = \frac{y''(x)}{\left(1 + y'(x)^2\right)^{3/2}}. \tag{14}$$

The curvatures of the three profiles will be denoted by κ_T, κ_C and κ_P. The curvature κ_T is necessarily computed with numerical methods. Thanks to [7], it suffices the derivatives of u up to the first order because

$$\kappa_T = \frac{1}{\sqrt{1 + u'^2}} \left(\frac{u'}{x} - \frac{1}{u} \right).$$

For the catenary and the parabola, the curvatures are calculated from [14] and the parameterizations [9] and [13] obtaining

$$\kappa_C(x) = \frac{c}{\cosh^2(cx)}, \qquad \kappa_P(x) = \frac{2c}{(1 + 4c^2x^2)^{3/2}}.$$

For the calculations of the mean curvature H, it will be utilized the property that H measures the normal curvatures along two orthogonal tangent directions, one of them coincides with the curvature of the generating curve. If the parameterization of the axisymmetric surface is $(x,\theta) \mapsto (x\cos\theta, x\sin\theta, y(x))$, then

$$H(x,\theta) = \frac{1}{2} \left(\kappa(x) + \frac{y'(x)}{x\sqrt{1 + y'(x)^2}} \right).$$

For the rotational tectum, $H = \frac{1}{2u\sqrt{1+u'^2}}$ thanks to [7]. For the candidate surfaces, the expression of $H(x,\theta)$ is computed using the parameterizations of the profile curves. Table 4 shows all these calculations.

It is important to notice that the symbol c has been used for catenaries and parabolas, as well as, catenary rotation surfaces and paraboloids. However, the parameters c are distinct, in general, for both curves and surfaces because c (and m) is determined by the initial conditions (boundary curve and surface area). The value of κ_T at $x = 0$ is $u''(0)$. By the L'Hôpital's rule, taking limits in [7] as $x \to 0$, we obtain $2u''(0) = 1/u(0)$, so $\kappa_T(0) = 1/(2u(0))$. In all the computations, the value $u(0) = z_0$ was fixed to be 1. In particular, $\kappa_T(0) = 1/2$.

6.2. Analysis of results and discussion

In order to show the behavior of all curvatures, it has been fixed the radius $R = 14$ in the hanging problem. Once the boundary curve Γ_R and the surface area A_0 have been fixed, let $\mathcal{C}_{c,m}$ and $\mathcal{P}_{c,m}$ be the catenary rotation surface and the paraboloid with the same initial data. Fig. 7 shows the plots of κ_T, κ_C and κ_P.

In the three surfaces, the curvatures have a maximum at the lowest point $x = 0$ and next, the curvature changes rapidly to be almost zero as

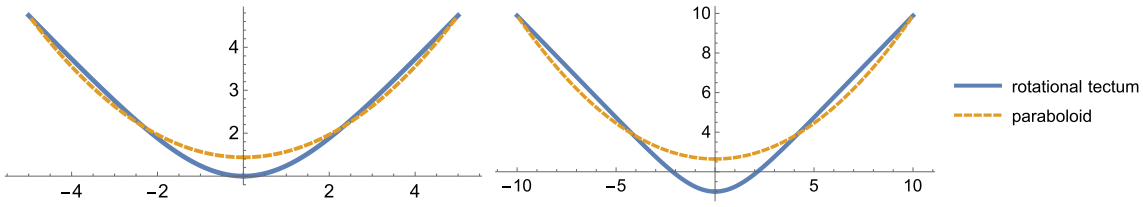

Fig. 6. Comparison between rotational tectums (thick) and paraboloids (dashed). Left: $R = 5$ where $h_T = 3.2115$, $h_P = 3.2219$ and $lw_P = 1.4387$. Right: $R = 10$, $h_T = 6.5477$ and $h_P = 6.5994$. Here $lw_P = 2.6442$.

$x \to \infty$. This is expected for the rotational tectum because u is asymptotic to the straight-line $z = x$ in the coordinate xz-plane (see final remarks in Section 3.2). However, κ_C and κ_P take values significantly lower than κ_T around the lowest point. The functions κ_C and κ_P look like coincident not only around $x = 0$ but in all its domain. The curvatures κ_C and κ_P go to 0 as $x \to \infty$ by the expressions of Table 4. However, the decay growth is different because for a catenary rotation surface, this decay is of type e^{-2cx} and for paraboloids of order x^{-3}.

For the mean curvature H, the behaviours of H_T, H_C and H_P along the profile curves are similar than the curvatures of the profile curves, because H gathers part of information from the curvature of the profile curve. For example, the inequalities $H_T > H_C$ and $H_T > H_P$ hold around the lowest point. Other property is that the mean curvatures H_C and H_P are almost identical in all its domain. All the mean curvatures converge to 0 as $x \to \infty$. Again, the type of decay between H_C and H_P is different.

As a conclusion, the curvature functions κ around the lowest point of the two candidate surfaces are close between them, but far from the mathematical model. In all them, the functions are decreasing along the profile curve (as one goes from $x = 0$ to $x = R$). The mathematical model presents a great contrast between $x = 0$ and $x = R$.

The previous analysis has been done for the value $R = 14$. For arbitrary R, it is interesting to investigate the values κ_C and κ_P for different values of R. See Table 5. At $x = 0$, $\kappa_C(0) = c$ and $\kappa_P(0) = 2c$ (different constants c). Just at the vertex, the value of the mean curvature coincides with that of κ. For the rotational tectum, $\kappa_T(0) = 1/(2z_0) = 1/2$.

Since the value $\kappa_T(0)$ is constant (equal to 0.5) the rate of increase is 0. However, for $\kappa_C(0)$ and $\kappa_P(0)$, the slopes of the linear regression line are $S_{lp} = -0.01118$ and $S_{lp} = -0.0165$, respectively. In order to give an adequate comparison, let us observe that the difference between both slopes is of 42%. This is in accordance with the different type of decays of the curvatures κ_C and κ_P previously explained. As a consequence, the value of the curvature of the catenary adjusts better than that of the parabola.

7. Conclusions

The aim of this paper was to investigate if catenary rotation surfaces and paraboloids are close or far from the mathematical model of a rotational dome. This objective has been achieved because the centers of gravity of these surfaces have been computed and subsequently, a comparative analysis of these calculations has been shown. Among the results, it is established that catenary rotation surfaces and paraboloids have both a high degree of approximation to the rotational tectum. On the other hand, it has been also demonstrated that paraboloids adjust better than catenary rotation surfaces.

The fact that the solutions of the singular minimal surface eq. (7) cannot be obtained by quadratures gives a great difficulty to use these surfaces in architecture when implementing them in practice. This leads to the idea of replacing the mathematical model with other mathematical surfaces that are easier to work with, but without losing, as far as possible, the property that characterizes the rotational tectums. This property is that the forces acting on the surface are only due to compression forces. It was therefore necessary to check the centers of gravity of the two candidate surfaces.

Catenary rotation surfaces and paraboloids are generated by two famous curves, the catenary and the parabola, respectively. These curves are well known in geometry, but also in architecture because both curves are created by funicular structures.

The accuracy of the two candidate surfaces with the rotational tectum is investigated by comparing their centers of gravity. The height of the center of gravity measures, up to physical constants, the energy of the rotational dome when it is subjected only to forces of compression. On the basis of the numerical results, the main consequence is that both surfaces are good approximations of the mathematical model. In both cases, the percentage errors of the slope of linear regression line are of 0.93 % and 0.41 %, being actually low percentages for both candidate surfaces.

A second result is that paraboloids adjust better than the catenary rotation surfaces. This conclusion has been tested using the slopes of the linear regression line of the heights of the centers of gravity in relation with the height of the mathematical model. Taking into account

Table 4
Curvatures κ and H along γ.

	$\mathcal{T}$	$\mathcal{C}_{c,m}$	$\mathcal{P}_{c,m}$
$\kappa(x)$	$\frac{u''}{(1+u'^2)^{3/2}}$	$\frac{c}{\cosh^2(cx)}$	$\frac{2c}{(1+4c^2x^2)^{3/2}}$
$\kappa(0)$	$\frac{1}{2u(0)}$	c	$2c$
$H(x)$	$\frac{1}{2u(x)\sqrt{1+u'(x)^2}}$	$\frac{1}{2}\left(\frac{c}{\cosh^2(cx)} + \frac{\sinh(cx)}{x\cosh(cx)}\right)$	$\frac{2c(1+2c^2x^2)}{(1+4c^2x^2)^{3/2}}$

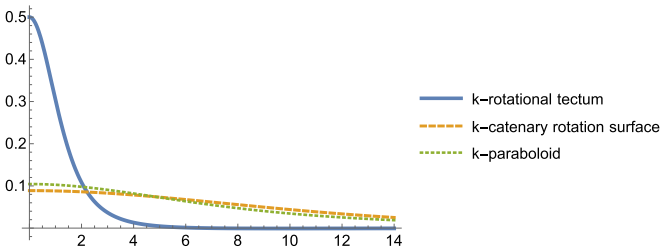

Fig. 7. Comparison between the curvatures κ of the profiles of the two candidate surfaces and the rotational tectum. Here $R = 14$.

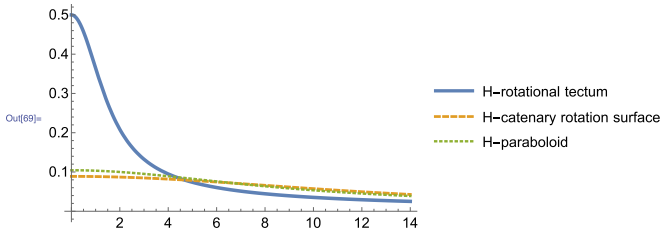

Fig. 8. Comparison between the mean curvatures H along the generating curves of the two candidate surfaces and the rotational tectum. Here $R = 14$.

Table 5
Values of κ_C and κ_P at the vertex $x = 0$ of the rotational surfaces for different values of R.

R	κ_T	$\kappa_C(0)$	$\kappa_P(0)$
2	0.5	0.3985	0.4268
4	0.5	0.2726	0.3091
6	0.5	0.1974	0.2288
8	0.5	0.1525	0.1782
10	0.5	0.1235	0.1448
12	0.5	0.1034	0.1215
14	0.5	0.0888	0.1044
16	0.5	0.0778	0.0914
18	0.5	0.0691	0.0813
20	0.5	0.0622	0.0731
$\mathbf{S_{lp}}$	0	−0.0118	−0.0165

both values, paraboloids clearly win to catenary rotation surfaces. To this, we add the clear advantage of paraboloids because they are more manageable from the computational viewpoint.

To the best of our knowledge, no research has been carried out to test the centers of gravity of catenary rotation surfaces and paraboloids. However, the paraboloid is an example of a well-studied surface in architecture. Some studies concerning to the stress, equilibrium conditions, elasticity and stress-strain state of paraboloids appear in [2,5,13,19,20,37]. In all these works, it has not been considered the center of gravity as a parameter that may useful in the construction of domes.

This paper has proved that paraboloids adjust reasonably well to the mathematical model of the rotational tectum. In consequence, our results would demonstrate that paraboloids can serve as good designs for construction of domes and cupolas.

CRediT authorship contribution statement

Rafael López: Conceptualization, Methodology, Formal analysis, Investigation, Visualization, Writing – original draft, Writing – review & editing.

Data availability

No data was used for the research described in the article.

Declaration of competing interest

I have nothing to declare with respect to competing interests.

Acknowledgments

The author thanks to the referees for their comments and suggestions, which have notably improved the presentation of this paper as well as a right discussion of the results. The author is a member of the Institute of Mathematics of the University of Granada. This work has been partially supported by the Projects I+D+i PID2020-117868GB-I00, A-FQM-139-UGR18 and P18-FR-4049.

Appendix A. Appendix

This appendix shows the *Mathematica* codes employed to obtain Tables 1 and 2. Similar codes are equally valid for the paraboloids in Section 5. The first input is the equation of the catenary [1]:

```
(* The equation of the catenary *)
z[x_]:=1/c Cosh[c x]+m
```

The next step is the description of the rotational tectum. For this, it is necessary to find a solution of eq. (7). This equation presents a singular point at $x = 0$. Thus the initial condition must be changed to be close to 0. In the present case, take $r_0 = 0.000001$. The initial conditions are $u(r_0) = z_0$, with $z_0 = 1$, and $u'(r_0) = 0$. The value of the radius of the boundary circle is R. In the next code lines, the input is $R = 2$. The function NDSolve is used to solve [7].

```
(* Solving the singular minimal surface equation *)
ro=0.000001;R=2;zo=1;sol=
NDSolve[ u"[x]/(1+u'[x]^2)+u'[x]/x==1/ u[x],
u[ro]==zo,u'[ro]==0, u[x],x,ro,R];
uu[x_]=u[x]/.sol[[1]];
```

The computation of the area A_0 of the rotational tectum uses the formula $2\pi\int_{r_0}^{R} x\sqrt{1+u'^2}\,dx$. The *Mathematica* function employed is `NIntegrate`.

```
(* area of the rotational tectum *)
Ao=NIntegrate[2Pi x Sqrt[1+uu'[x]^2],x,ro,R]
```

The value of the height of the center of gravity of the rotational tectum is calculated with the formula $\frac{2\pi}{A_0}\int_{r_0}^{R} xu\sqrt{1+u'^2}\,dx$:

```
(* height of the center of gravity of the rotational tectum *)
hT=NIntegrate[2Pi uu[x]x Sqrt[1+uu'[x]^2],x,ro,R]/Ao
```

With the value A_0, the parameters c and m of the catenary $\mathcal{C}_{c,m}$ are calculated thanks to [10] and [11]. In *Mathematica*, the function to use is FindRoot.

```
(* Finding the parameters c and m for the rotational catenary *)
variables=
FindRoot[z[R]==uu[R],
2Pi (c R Sinh[c R]-Cosh[c R]+1)/c^2==Ao,c,.3,m,-4];
```

The computation of the height h_C of the center of gravity of the catenary rotation surface uses the formula (12).

```
(* height of the center of gravity
of the rotational catenary *)
hC=
Pi (2 c^2 R^2+2 c R Sinh[2 c R]-Cosh[2 c R]+1)/
(4 c^3 Ao)+m/.variables
```

Finally it is computed the deviation of the value h_C with h_T in relation with the height of the rotational tectum.

```
(*deviation with respect to the height of the surface *)
(hC-hT)/(uu[R]-1) 100
```

References

[1] Animasaun IL, Ibraheem RO, Mahanthesh B, Babatunde HA. A metaanalysis on the effects of haphazard motion of tiny/nano-sized particles on the dynamics and other physical properties of some fluids. ChinJPhys. 2019;60:676–87.
[2] Banerjee SP. Analysis of elliptic-paraboloid shell. JStructDiv. 1968;94:2213–30.
[3] Beltrami E. Sull equilibrio delle superficie flessibili ed inestensibili, 3. Memorie della Academia delle Scienze dell Istituto di Bologna, Series 4; 1882. p. 217–65.
[4] Benvenuto E. An introduction to the history of structural mechanics. New York: Springer; 1991.
[5] Blaauwendraad J, Hoefakker JH. Hyperbolic and elliptic-paraboloid roofs. Structural shell analysis. Solid mechanics and its applications. Dordrecht: Springer; 2014.
[6] Böhme R, Hildebrandt S, Taush E. The two-dimensional analogue of the catenary. PacJMath. 1980;88:247–78.
[7] Como M. Statics of historic masonry constructions. Berlin, Germany: Springer; 2017.
[8] Cowan HJ. A history of masonry and concrete domes in building construction. Build Environ. 1977;12:1–24.
[9] Dierkes U. Minimal hypercones and C0,1/2 minimizers for a singular variational problem. Indiana UnivMathJ. 1988;37:841–63.
[10] Dierkes U. Singular minimal surfaces. In: Hildebrandt S, Karcher H, editors. Geometric analysis and nonlinear partial differential equations. Berlin: Springer; 2003. p. 177–93.
[11] Dierkes U, Groh N. Symmetric solutions of the singular minimal surface equation. AnnGlobAnalGeom. 2021;60:431–53.

[12] Dierkes U, Huisken G. The -dimensional analogue of the catenary: existence and nonexistence. PacJMath. 1990;141:47–54.
[13] Du W, Zhu Z, Zhu L. Comparison of four structural schemes for the roof design of Qinyang Stadium. Appl Mech Mater. 2013;438–439:819–23.
[14] Germain S. Recherches sur la théorie des surfaces elastiques. Paris: Veuve Courcier; 1821.
[15] Heyman J. On shell solutions for masonry domes. IntJSolidsStruct. 1967;3:227–41.
[16] Heyman J. The stone skeleton. Structural engineering of masonry architecture. Cambridge: Cambridge University Press; 1995.
[17] Huerta S. Structural design in the work of gaud. ArchitSciRev. 2006;49:327–39.
[18] Jellet JH. On the properties of inextensible surfaces. Trans R Irish Acad. 1853;22: 343–78.
[19] Kollár L, Tarján G. Mechanics of civil engineering structures. Duxford: Elsevier; 2021.
[20] Krivoshapko SN, Gbaguidi-Aisse GL. Geometry, static, vibration and buckling analysis and applications to thin elliptic paraboloid shells. Open ConstrBuildTechnolJ. 2016;10:576–602.
[21] Kurre KE. The history of the theory of structures: searching for equilibrium. 2nd edn. Wilhelm Ernst and Sohn Verlag für Architectur und technische Wissenschaften GmbH. Co. KG; 2018.
[22] Lagrange JL. Mécanique analytique. Tome XI. 4th ed. Paris: Gauthier-Villars; 1888.
[23] Lluis i Ginovart J, Coll-Pla S, Costa-Jover A, Piquer MLópez. Hooke's chain theory and the construction of catenary arches in Spain. Int J Archit Herit. 2017;11:703–16.
[24] López R. Invariant singular minimal surfaces. AnnGlobAnalGeom. 2018;53:521–41.
[25] López R. Uniqueness of critical points and maximum principles of the singular minimal surface equation. JDifferEqu. 2019;266:3927–41.
[26] López R. Compact singular minimal surfaces with boundary. AmJMath. 2020;142: 1771–95.
[27] R. López, Plateau-Rayleigh instability of singular minimal surfaces. Comm. Pure Appl. Anal., to appear.
[28] Mainstone R. Developments in structural form. Routledge; 2013.
[29] Mitchell WJ. Computer aided architectural design. New York: Van Nostrand Reinhold; 1977.
[30] Nikolić D. Catenary arch of finite thickness as the optimal arch shape. StructMultidiscipOptimiz. 2019;60:1957–66.
[31] Nitsche JCC. A nonexistence theorem for the two-dimensional analogue of the catenary. Analysis. 1986;6:143–56.
[32] Otto F. Zugbeanspruchte Konstruktionen. Bd. I, II. Berlin, Frankfurt, Wien: Ullstein; 1962/1966.
[33] Poisson SD. Mémoire sur les surfaces élastiques. Mémoires de l'Institut de France, Vol. 9. ; 1814/1816. p. 167–226.
[34] Radford AD, Gero JS. On optimization in computer aided architectural design. Build Environ. 1980;15:73–80.
[35] Schmitt G. Architectura et machina: computer aided architectural design und virtuelle architektur. Springer-Verlag; 2013.
[36] Schodek DL, Bechthold M. Structures. Pearson Higher Ed.; 2013
[37] Scrivener JC. The analysis of elliptic and hyperbolic paraboloid shell roofs. NZEng. 1964;19:303–10.
[38] Shah NA, Animasaun IL, Ibraheem RO, Babatunde HA, Sandeep N, Pop I. Scrutinization of the effects of Grashof number on the flow of different fluids driven by convection over various surfaces. J Mol Liq. 2018;249:980–90.
[39] Truesdell C. The membrane theory of shells of revolution. TransAmMathSoc. 1945; 58:96–166.
[40] Wakif A, Animasaun IL, Satya Narayana PV, Sarojamma G. Meta?analysis on thermo? migration of tiny/nano?sized particles in the motion of various fluids. ChinJ Phys. 2019;68:293–307.
[41] Wikipedia contributors. The free encyclopedia. Colegio Teresiano de Barcelona. https://es.wikipedia.org/w/index.php?title=Colegio_Teresiano_de_Barcelona_oldid=134544852.
[42] Wikipedia contributors. The free encyclopedia. Maqueta funicular de la cripta de la colonia Güell. https://es.wikipedia.org/w/index.php?title=Maqueta_funicular_de_la_cripta_de_la_colonia_G%C3%BCell&oldid=134388617.
[43] Wolfram Research Inc. Mathematica, version 13.0; 2021. Champaign, IL.